

Paleomagnetic Investigation of McMurdo Volcanics, Antarctica

Minoru FUNAKI*

マクマード火山岩類の古地磁気

船 木 實*

要旨: 合計 212 個の古地磁気学用試料を、マクマードサウンドのハットポイント半島、ロイズ岬、およびテイラー谷から採集した。これらの試料は安定な自然残留磁気を持つことが確かめられ、以下に述べるような結果が得られた。(1)南極大陸は少なくとも鮮新世末期に、現在の南極大陸の位置にあった。鮮新世末期から現代に至るまでの磁極の移動範囲は(正帯磁: 11地点, 逆帯磁: 3地点), 半径 30° の南極域内で、その中心位置は、現在の南極点の近くにあった。(2)この地域の溶岩の流出順序は、古地磁気学、地質学、それに年代学の結果を総合して、新しいものから古い順に、次のように推定される。ツインクレーターとロイズ岬(ブリュンス期)、ハーフムーンクレーター(ハラミロ・イベント)、オブザベーションヒルとアーミテージ岬(松山期)、クレーターヒルとキャッスルロック(オルデュバイあるいはレユニオン・イベント)、テイラー谷(カエナ・イベント)。

Abstract: A total of 212 paleomagnetic samples were collected from the Hut Point Peninsula, the Cape Royds and the Taylor Valley in the McMurdo Sound, Antarctica. These samples have stable natural remanent magnetization. The results of paleomagnetic studies are as follows: (1) The position of Antarctica has been almost the same from the Late Pliocene Age up to the present. The position of the virtual geomagnetic pole (VGP) (11 normals and 3 reverses) from the Pliocene Age to the present is within a polar cap area of about 30° latitude, whose center is located almost exactly at the south geographical pole. (2) The sequence of lava eruption was determined by synthetic evidence from paleomagnetic, geological and geochronological data. The result revealed, from the latest to the earliest, Twin Crater Sequence and Cape Royds Sequence (Brunhes Epoch), Half Moon Crater Sequence (Jaramillo Event), Observation Hill Sequence, Cape Armitage Sequence (Matuyama Epoch), Crater Hill and Castle Rock (Olduvai or Réunion Events) and Taylor Valley Sequence (Kaena Event).

1. Introduction

The McMurdo Sound area in the Ross Sea has a wide ice-free area along the coast line of the South Victoria Land, especially in the Dry Valley region (*i.e.*, Victoria Valley, Wright Valley and Taylor Valley). From the late Tertiary to the Quaternary volcanic activity took place, resulting in the emergence of the McMurdo volcanics across large areas of the Ross Sea and the Transantarctic Mountains.

* 国立極地研究所, National Institute of Polar Research, 9-10, Kaga 1-chome, Itabashi-ku, Tokyo 173.

Paleomagnetic investigations of Cenozoic volcanics in the Hut Point Peninsula, Ross Island, were carried out by COX (1966), MCMAHON and SPALL (1974a, b), KYLE and TREVES (1974), ARMSTRONG (1978) and FUNAKI (1979). COX (1966) reported that surface samples of trachyte from the Observation Hill, the tip of the Hut Point Peninsula, were found to be reversely magnetized, whereas the majority of lava flows and cones in the McMurdo Sound showed normal magnetization. MCMAHON and SPALL carried out paleomagnetic studies of Core No. 1 (196.54 m long) and Core No. 2 (171.38 m long) obtained during the Dry Valley Drilling Project (DVDP), as shown in Fig. 1, and reached the general conclusion that natural remanent magnetizations (NRM's) of all samples of No. 1 and No. 2 cores, except those of a layer of 1 m in thickness, show Matuyama reverse polarity, and predate the Jaramillo event (0.89 to 0.95 m.y.), the average inclination of NRM being -83° (downward magnetization in the Southern Hemisphere). They examined the NRM stability of pilot samples of No. 2 core, and found that the samples possessed a very stable magnetization direc-

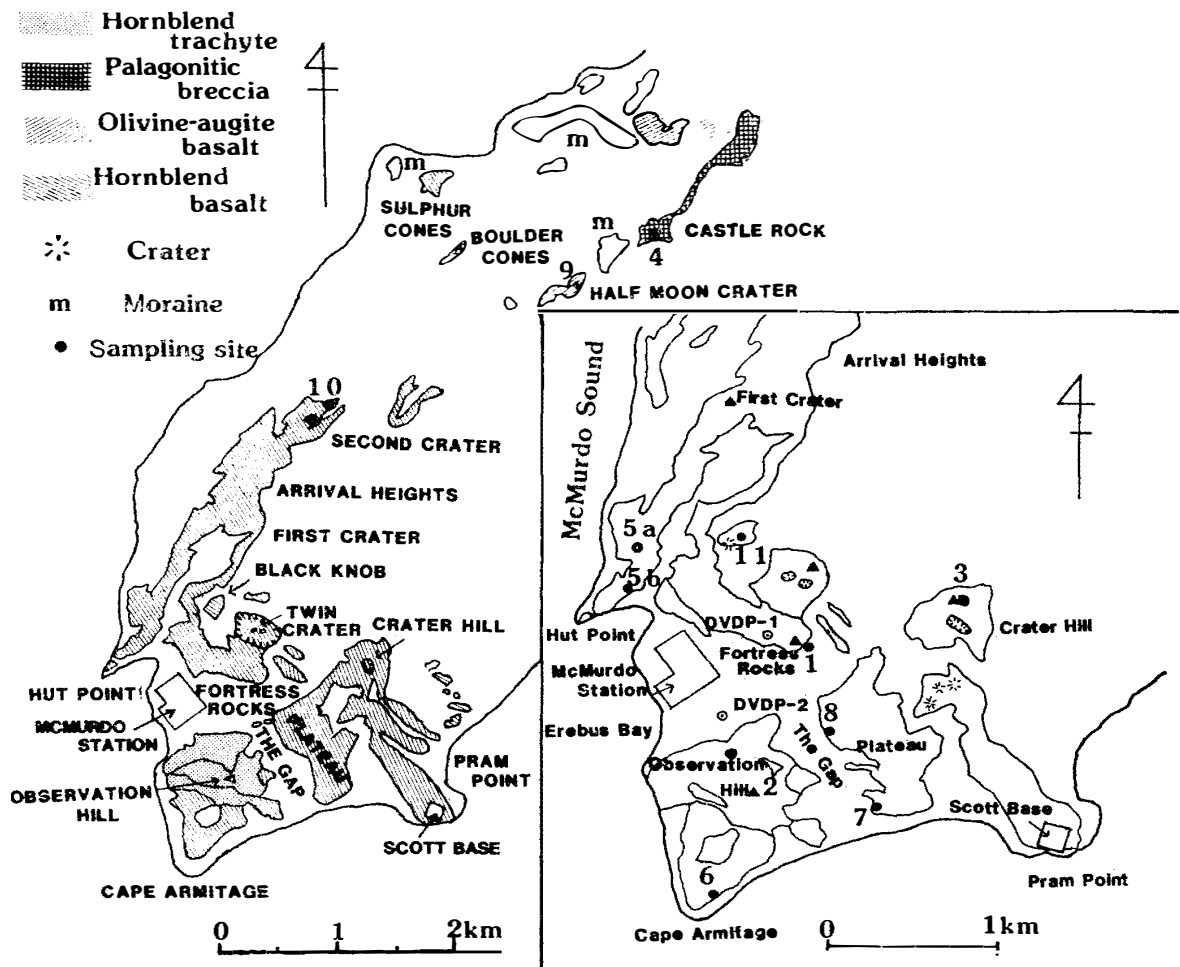


Fig. 1. Sampling sites and geological map (COLE et al., 1971) of Hut Point Peninsula. The names of sampling sites are as follows. 1. Fortress Rocks. 2. Observation Hill. 3. Crater Hill. 4. Castle Rock. 5a. North of Hut Point. 5b. Near Hut Point. 6. Cape Armitage. 7. Site between Cape Armitage and Scott Base. 8. East of The Gap. 9. Half Moon Crater. 10. Second Crater. 11. Black Knob.

tion. KYLE and TREVES (1974) measured the NRM to decide the volcanic sequence of 5 rock masses collected from the Hut Point Peninsula, *i.e.*, Twin Crater, Second Crater, Half Moon Crater, Observation Hill, and lava flows 250 m north of Scott Base (see Fig. 1). However, these samples were not magnetically clean. ARMSTRONG (1978) reported that late Cenozoic basalts are magnetized in the normal direction (at Half Moon Crater in the Hut Point Peninsula), but reversely magnetized in the Taylor Valley, except for one site. FUNAKI (1979) studied the area of drift of the south geomagnetic pole using ten rock masses collected from the Hut Point Peninsula. His results show that the position of the virtual geomagnetic pole (VGP) (8 normals and 2 reverses) is within a polar cap area of about 30° latitude. However, the NRM stability is not fully discussed in this study.

2. Geology and Sampling

Volcanic cones and lava flows may be observed at the tip of the Hut Point Peninsula. These volcanics consist of basanite and basanitoid with a smaller amount of hawaiite and phonolite. Most of the volcanic cones are concentrated on a prominent lineation whose strike is NNE along the western side of the peninsula. The late Quaternary surface geology of this area has been described by WELLMAN (1964), COLE *et al.* (1971) and KYLE and TREVES (1973). Figure 1 shows the geology of the Hut Point Peninsula as summarized by COLE *et al.* (1971). Studies of the subsurface geology in this area were carried out by DVDP, and the results were reported by TREVES and KYLE (1973). KYLE and TREVES (1974) summarized the relationships between surface and subsurface geology based on paleomagnetic and chronological data. According to these results, the inferred eruptive sequence for the Hut Point Peninsula is as follows: first a very early pile of palagonitic breccias (Castle Rock Sequence); olivine-augite basalt (Crater Hill Sequence); hornblende trachyte (Observation Hill Sequence); hornblende basalt (Half Moon Crater Sequence); and finally a later olivine-augite basalt (Twin Crater Sequence). According to the results of analyses of DVDP No. 1, 2 and 3 cores, these cores are assigned to five stages in the sequence of volcanic activity, namely, from the latest to the earliest, Twin Crater, Half Moon Crater, Observation Hill, Crater Hill and the palagonitic breccia of Castle Rock (TREVES and KYLE, 1973; KYLE and TREVES, 1974). The palagonitic breccia of Castle Rock is thought to be of submarine or subglacial origin (KYLE and TREVES, 1974).

The volcanic rock at the Cape Royds consists of at least three major kentyte flows which are partially mantled by volcanic agglomerate, breccia and lithic tuff (TREVES, 1962).

Relatively small volcanic eruptions took place during the Pleistocene period in the Taylor Valley, and the rock types are similar to late cinder cones at the Cape Armitage (ANGINO *et al.*, 1962). HARRINGTON (1958) reported that the volcanic rocks in the Taylor Valley are fragments of the McMurdo volcanic rocks.

Chronological data for the McMurdo volcanics at the Hut Point Peninsula, Cape Royds and Taylor Valley are summarized in Table 1. The K-Ar ages of lavas from Black Knob, southwest of Black Knob, Half Moon Crater, Observation Hill, and the

Table 1. Chronological data at Hut Point Peninsula, Cape Royds and Taylor Valley.

Sampling site		K-Ar age (m.y.)	Reference
Hut Point Peninsula	Black Knob	0.43 ± 0.07	ARMSTRONG (1978)
	Southwest of Black Knob	0.58 ± 0.03	"
	Half Moon Crater	1.0 ± 0.15	"
	Castle Rock dyke	1.1 ± 0.4	KYLE and TREVES (1974)
	Observation Hill	1.18 ± 0.03	FORBES <i>et al.</i> (1974)
Cape Royds		0.68 ± 0.14	TREVES (1967)
Taylor Valley (below Marr Glacier)		2.93 ± 0.10	ARMSTRONG (1978)
"		2.89 ± 0.10	"
"		2.87 ± 0.15	"

dyke of Castle Rock have been determined as 0.43 ± 0.07 , 0.58 ± 0.03 , 1.0 ± 0.15 , 1.18 ± 0.03 and 1.1 ± 0.4 m.y. respectively (ARMSTRONG, 1978; KYLE and TREVES, 1974; FORBES *et al.*, 1974). TREVES (1967) reported that the K-Ar age of anorthoclase from the Cape Royds area is 0.68 ± 0.14 m.y. In the Taylor Valley, the age of basaltic rock from our sampling sites was reported to be 2.93 ± 0.10 and 2.87 ± 0.15 m.y. by ARMSTRONG (1978).

In the 1977-79 austral summer seasons, rock samples were collected from the Hut Point Peninsula and the Cape Royds in Ross Island and from the Taylor Valley. The sampling sites in the Hut Point Peninsula are illustrated in Fig. 1; they are (1) Fortress Rocks, (2) Observation Hill, (3) Crater Hill, (4) Castle Rock, (5a) North of Hut Point, (5b) Near Hut Point, (6) Cape Armitage, (7) Site between Cape Armitage and Scott Base, (8) East side of The Gap, (9) Half Moon Crater, (10) Second Crater, and (11) Black Knob. At Cape Royds, the samples were collected at two sites; one (12), Cape Royds A, is 300 m northeast of Shackleton Hut, and the other (13), Cape Royds B, is 1000 m north of the Hut. In the Taylor Valley, the samples (14) were collected from basaltic cones under the Marr Glacier in the middle of the valley.

The direction of the samples was checked using a Sun compass. Paleomagnetic specimens, 1 inch in both diameter and length, were cut out in the laboratory from each rock mass collected from 15 sites.

3. Experimental Results

3.1. Magnetic hysteresis properties

The magnetic hysteresis properties of typical samples from each site, except (4), were measured using a vibrating sample magnetometer at room temperature. The applied external field intensity was found to be between -15.5 and 15.5 kG. Saturation magnetization (I_s), saturation remanent magnetization (I_R), coercive force (H_c) and remanent coercive force (H_{RC}) are summarized in Table 2 together with the intensity of natural remanent magnetization (I_n), and the ratios of I_n/I_s and I_R/I_s .

The ratio of I_n/I_s for all samples ranges from 0.92×10^{-3} to 5.590×10^{-3} , except for (3), (8), (9) and (14). The ratios for (3) and (9) are as large as 13.113×10^{-3} and

Table 2. Basic magnetic properties of volcanic rocks from McMurdo Sound.

Sample name	I_n NRM (emu/g)	I_s (emu/g)	I_R (emu/g)	H_c (Oe)	H_{RC} (Oe)	I_n/I_s ($\times 10^{-3}$)	I_R/I_s	I_s-T			
								Type	Heating curve (°C)	Cooling curve (°C)	
Hut Point Peninsula	1. Fortress Rocks	1.53×10^{-3}	0.79	0.108	30	74	1.938	0.137	1	~115	~100
	2. Observation Hill	1.34×10^{-3}	1.45	0.26	205	441	0.924	0.179	3	580	555
	3. Crater Hill	5.14×10^{-3}	0.39	0.125	152.5	320	13.113	0.321	4	560, ~310*	560, ~290*
	5a. North of Hut Point	6.04×10^{-3}	1.83	0.608	305	487	3.302	0.332	5	570, 40*	530, 40*
	5b. Near Hut Point	6.99×10^{-3}	1.25	0.285	80.5	270	5.590	0.228	5	540, ~120*	525, ~120*
	6. Cape Armitage	2.30×10^{-3}	1.50	0.178	59	243	1.531	0.119	6	475, ~130*	~100
	7. Between Cape Armitage and Scott Base	2.81×10^{-5}	0.017	0.0018	78.5	520	1.654	0.106	2	~-40, 20*	~-40, ~20*
	8. East side of The Gap	1.70×10^{-6}	0.009	0.0027	73.5	363	0.189	0.300	2	-25, ~100*	-25, -100*
	9. Half Moon Crater	3.71×10^{-3}	0.156	0.027	44	68	23.782	0.173	4	550, ~290*	520, ~290
	10. Second Crater	3.52×10^{-3}	1.15	0.17	75	152	3.062	0.148	3	510	510
	11. Black Knob	2.12×10^{-5}	0.014	0.004	129	510	1.515	0.286	2	-20, ~100*	-20, ~100*
12. Cape Royds A	1.17×10^{-3}	0.430	0.080	68.5	188	2.719	0.186	5	570, ~100*	550, ~100	
13. Cape Royds B	1.16×10^{-4}	0.295	0.051	66	123	0.393	0.173	5	~120, 550*	~120, 550*	
14. Taylor Valley (normal polarity)	1.58×10^{-3}	2.87	0.49	175	442	0.551	0.171	3	555	520	
Taylor Valley (reversed polarity)	4.06×10^{-4}	2.12	0.34	128	528	0.192	0.160	5	560, ~250	540, ~130	

* sub-Curie point.

23.782×10^{-3} respectively, whereas those of (8) and (14) are 0.189×10^{-3} and 0.551×10^{-3} respectively. However the ratio of I_R/I_s ranges from 0.106 to 0.332 in all samples. The dispersion of I_R/I_s is much smaller than that of I_n/I_s . Therefore, the intensity of NRM may be classified into three groups, *i.e.*,

$$I_n/I_s > 10^{-2}, \quad 6 \times 10^{-3} > I_n/I_s > 4 \times 10^{-4} \quad \text{and} \quad I_n/I_s < 2 \times 10^{-4}.$$

The ranges of H_c and H_{RC} for all samples except (1) and (9) are from 59 to 305 Oe and from 123 to 528 Oe respectively. However, H_c values are 30 Oe and 44 Oe and H_{RC} values are 74 Oe and 68 Oe for (1) and (9) respectively. Most pilot samples are likely to have stable remanence, as their ferromagnetic constituents have a single or pseudosingle domain structure; but the stability of remanence may be a little worse for (1) and (9), as their ferromagnetic components have a pseudo-single or multi domain structure.

3.2. Thermomagnetic analyses

The thermomagnetic curves (I_s - T curve) of pilot samples from each site, except the samples from (4), were measured using a vibrating sample magnetometer from -269°C to 640°C in an external field of 5 kOe. A temperature range from -269°C to 50°C was obtained with a cryostat using liquid helium, and a higher temperature, from room temperature to 640°C , was obtained in 4×10^{-4} torr atmospheric pressure. The heating and cooling rates are $200^\circ\text{C}/\text{h}$.

Six typical I_s - T curves are shown in Fig. 2. Most of the heating and cooling curves are not exactly identical with each other, which suggests a change in composition during heating. I_s - T curves may be represented by using the sum of ferromagnetic magnetization, antiferromagnetic magnetization and paramagnetic magnetization. All I_s - T curves have a noticeable increase in magnetization below -200°C . The increase in magnetization is due to paramagnetic magnetization of Fe^{2+} in pyroxenes, olivines, ilmenites and other Fe^{2+} -bearing minerals (NAGATA *et al.*, 1972). Experiments have been made to try and detect the Néel point of ilmenite ($\theta = 57$ K), if any, but no evidence of the presence of ilmenite has been detected in the I_s - T curves of these samples.

The I_s - T curve can be divided into the following categories based on thermal reversibility. Type 1: reversible with single Curie point at 115°C . Type 2: reversible with not well-defined Curie point from 20°C to 150°C and one Curie point below 0°C . Type 3: almost reversible with single Curie point at 570°C . Type 4: comparatively reversible with two Curie points and increased magnetization after heating. Type 5: comparatively irreversible with two distinct Curie points and decreased magnetization after heating. Type 6: irreversible with two distinct Curie points, main Curie point being lowered and magnetization decreasing in cooling curve. The type of I_s - T curve and Curie points of each pilot sample are listed in Table 2 and typical examples of 6 I_s - T curves are illustrated in Fig. 2. The I_s - T curve from (1) is classified as Type 1. The curve shows a peculiar form, resembling Néel's *P*-type; magnetization has a peak at about -50°C and decreases from this point. AKIMOTO *et al.* (1957) reported that this remarkable I_s - T curve has a content of TiFe_2O_4 of more than 60%. In fact, since the observed Curie point of (1) is at about 115°C , the mol percent of TiFe_2O_4 may be estimated at about 70% using the TiFe_2O_4 - Fe_3O_4 diagram

(AKIMOTO *et al.*, 1957). The I_s - T curve of the samples collected from (7), (8), and (11) are classified as Type 2. In this case, no well-defined Curie point is observed in the range from $\sim -40^\circ\text{C}$ to $\sim 100^\circ\text{C}$ in the heating and cooling curves; titanium-rich titanomagnetites of varying composition are the inferred ferromagnetic minerals. The I_s - T curve of the samples collected from (2), (10) and (14) (normal polarity) are classified as Type 3. The observed distinct Curie point is the only one in the range

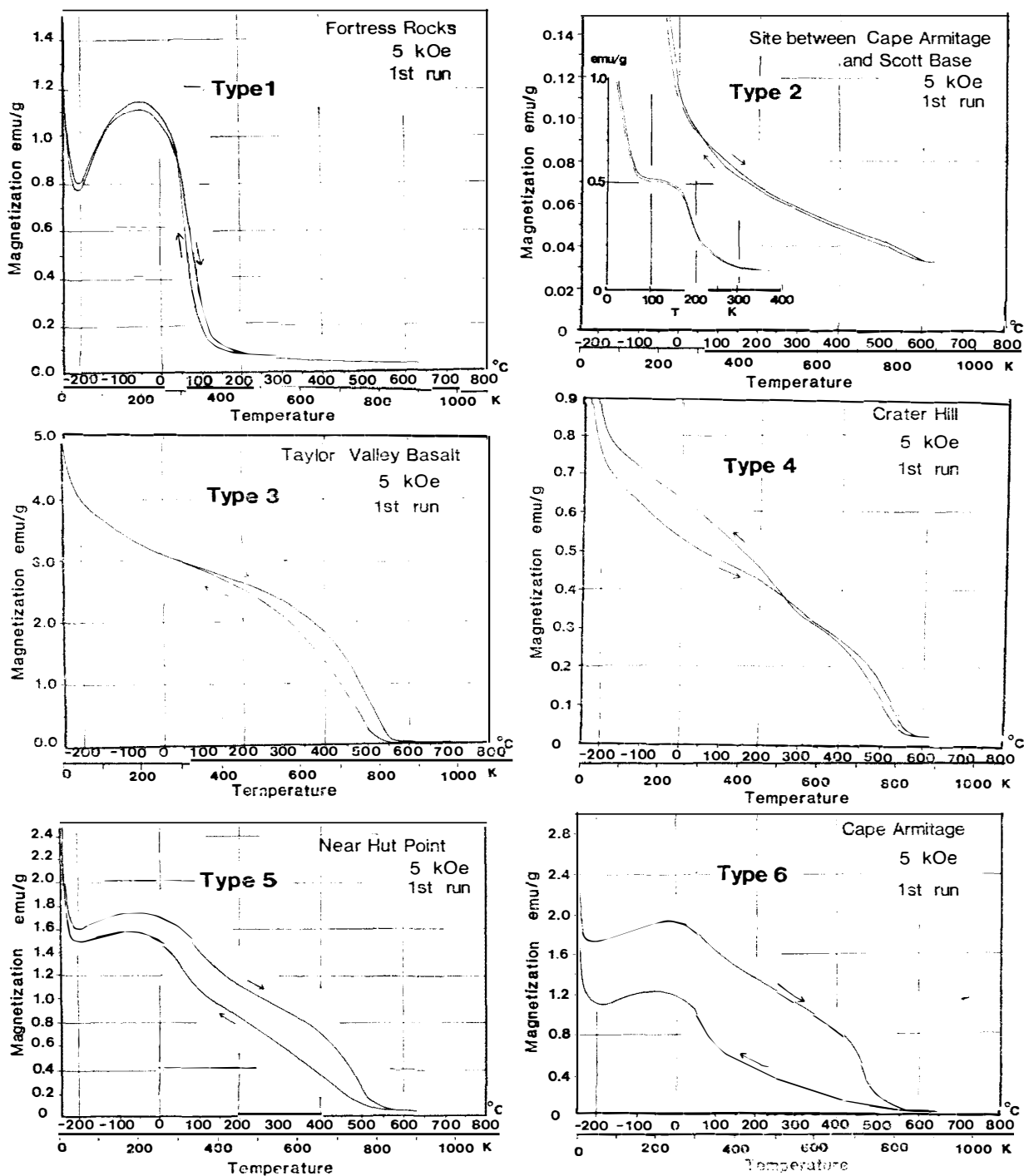


Fig. 2. Typical thermomagnetic curves (I_s - T curve) of six types from McMurdo volcanics.

from 580°C to 510°C. The inferred composition of ferromagnetic minerals is almost pure magnetite of constant composition. I_s - T curves of the samples collected from (3) and (9) are classified as Type 4. The I_s - T curve, with observed Curie point at ~560°C and ~300°C, is comparatively reversible as a whole. However, it is irreversible under ~300°C, due to magnetization increases in the cooling curve below 300°C. In this case, two kinds of ferromagnetic mineral are inferred, probably almost pure magnetite and titanomagnetite. I_s - T curves of the samples collected from (5a), (5b), (12), (13) and (14) (reversed polarity) are classified as Type 5. The observed Curie point in this type occurs from 540°C to 570°C and from 40°C to 250°C in the heating curve and from 550°C to 530°C and 130°C to 40°C in the cooling curve. The main Curie points range from 570~530°C; however, in the case of (13) it occurs at about 120°C with a sub-Curie point at 550°C. Thermomagnetic curves of samples collected from (5a) and (5b) are very similar to each other. The ferromagnetic minerals in this type may be inferred to be almost pure magnetite and titanomagnetite of constant composition, part of them may change to titanomaghemite or maghemite. The typical irreversible I_s - T curve of a sample collected from (6) is classified as Type 6. The observed Curie points are from 475°C to 570°C in the heating curve and ~100°C in the cooling curve. Since both the Curie point and magnetization decrease clearly in the cooling curve, part of the titanomagnetite may change to titanomaghemite (LARSON *et al.*, 1969).

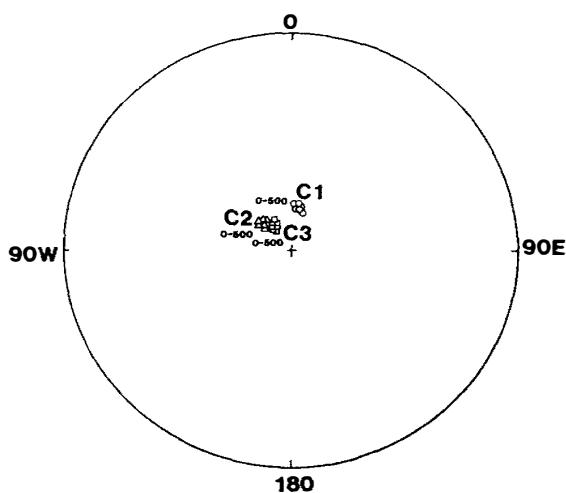
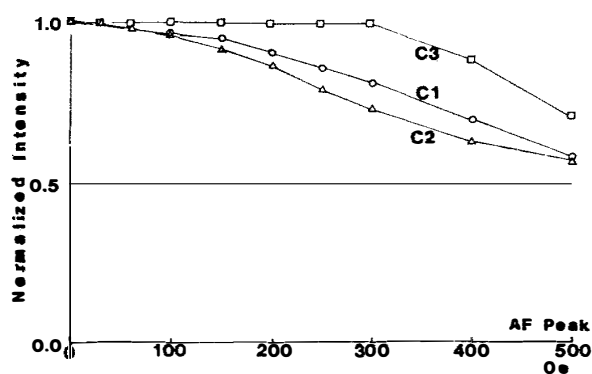


Fig. 3a.

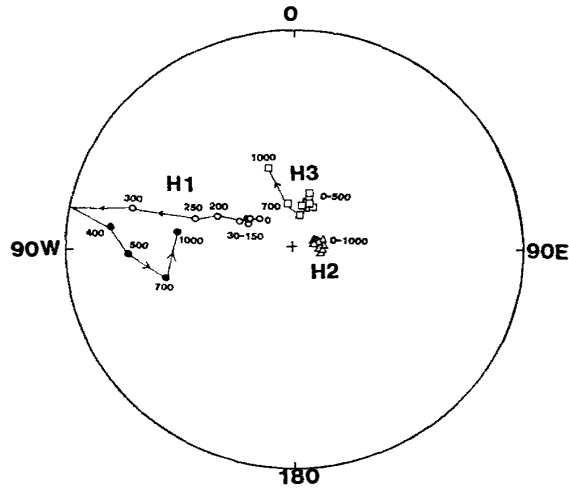
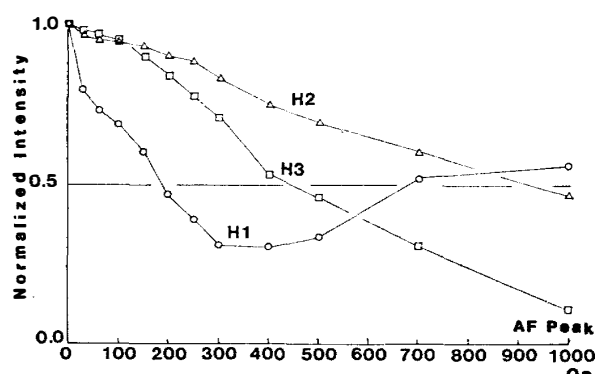


Fig. 3b.

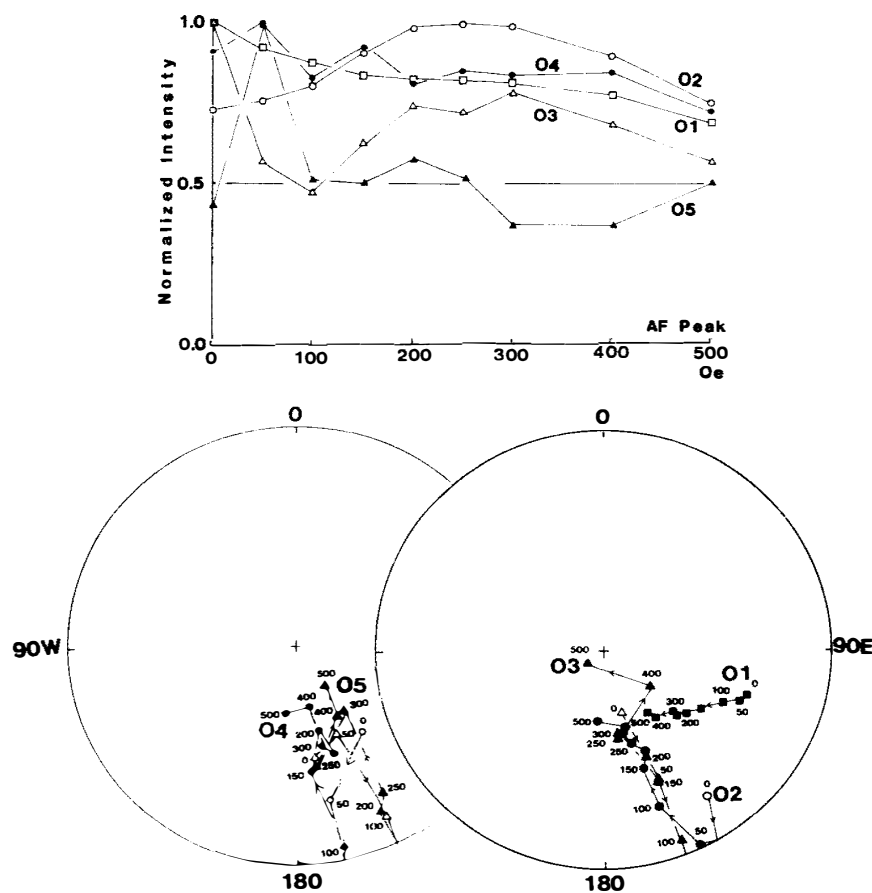


Fig. 3c.

Fig. 3. Representative AF demagnetization curves. Equal-area projection.
 (a) Crater Hill, (b) East side of The Gap and (c) Taylor Valley.

3.3. AF demagnetization of NRM

The pilot samples were demagnetized by steps, up to a peak of 500 or 1000 Oe using the alternating field (AF) demagnetization. The AF demagnetizer consists of a two-axis tumbler and a triple-layer Mumetal shield to cancel the effect of the earth's magnetic field.

Generally, the AF demagnetization of the intensity of NRM of all pilot samples, except those from (8) and (14), are very stable, usually the decay curve of intensity decreases gradually up to a peak of 500 Oe. Figure 3a shows a representative AF demagnetization curve of stable NRM. The values of the median demagnetization field (MDF) exceed the 200 Oe peak for all pilot samples. These directions of NRM are also very stable showing a peak of at least 500 Oe.

The NRM of matrix samples of palagonitic breccia from (4), originating in depositional remanent magnetization (DRM) or post-depositional remanent magnetization (pDRM), is very stable when AF demagnetization of both the intensity and the direction is applied. On the other hand, one (H1) of the three pilot samples from (8) is unstable against AF demagnetization, as shown in Fig. 3b; the intensity decreases gradually up to 350 Oe and then increases up to 1000 Oe. The direction is almost unchanged up to 150 Oe. However, the slope becomes shallow and then positive at 400 Oe. As shown in Fig. 3b, the NRM of the other two samples (H2

and H3) are stable at least up to 500 Oe. The AF demagnetization curves of the samples from (14) are shown in Fig. 3c. The intensity of the NRM of the reversed magnetized sample (O1) is very stable up to 500 Oe, but the direction of NRM is unstable up to 500 Oe. The NRM of the samples, from magnetized to normal direction, (O2, O3, O4, and O5), appears very unstable both in intensity and direction against AF demagnetization. The direction of NRM shifts from normal to reversed polarity with AF demagnetization. A minimum value is observed in the intensity of the decay curve when the direction is turned towards the horizon by AF demagnetization, and intensity is increased gradually up to 200–300 Oe. It seems that the direction of NRM is clustered into the best grouping when the demagnetizing field is about 350 Oe.

3.4. Microscopic observation

All pilot samples were polished for metallic microscopic observation under reflected light. Minerals of ferromagnetic grain and structure are distinguished by

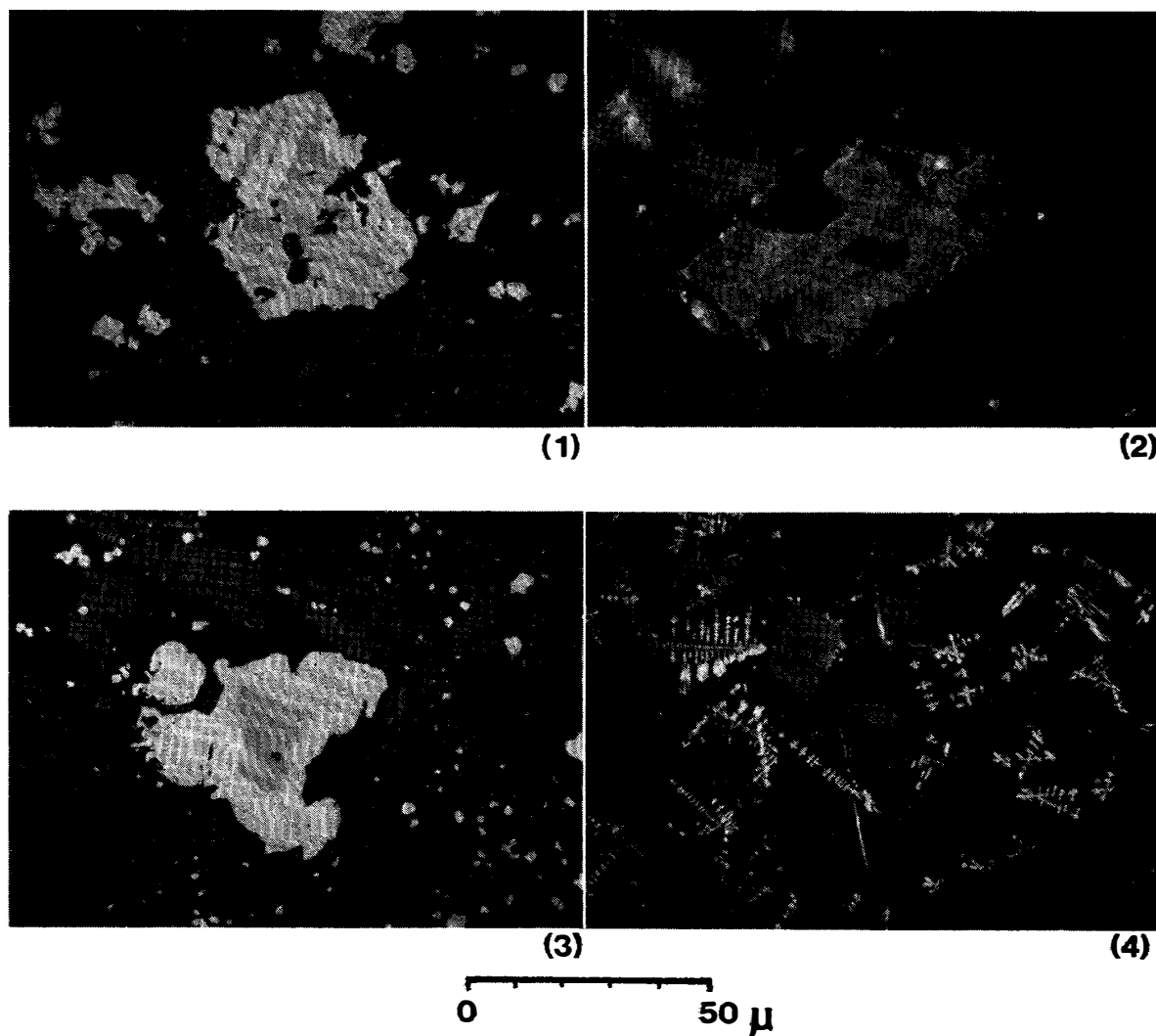


Fig. 4. Photomicrographs of typical titanomagnetite grains under reflected light. (1) Taylor Valley (normal polarity), coarse ilmenite lamella. (2) Observation Hill, fine ilmenite lamella. (3) Cape Armitage, titanomaghemite. (4) North of Hut Point, skeletal grain.

color, optical anisotropy, and shape of the grains.

The range of diameter of representative magnetic grains in all pilot samples under the microscope is less than $30\ \mu$, and the maximum diameter ranges from $40\text{--}300\ \mu$. The main magnetic mineral is identified as hematite for samples from (3) and (9) and as titanomagnetite or magnetite for samples from the other 12 sites excluding (14). In the case of (14), hematite grains and titanomagnetite grains with ilmenite lamellas coexist in reversed samples. However, the main ferromagnetic grains are titanomagnetite in the normal samples. The ilmenite lamellas are shown in Fig. 4(1) and (2); high temperature oxidation was observed in all titanomagnetite grains in samples from (2) and reversed samples from (14), and in some of the titanomagnetite grains in samples from (5a), (5b) and (10). Titanomagnetite low temperature oxidation is observed in some grains in the sample from Cape Armitage, as shown in Fig. 4(3). In the case of (5a), (5b), (10) and (11) skeletal grains of titanomagnetite of $10\text{--}20\ \mu$ in length were observed as shown in Fig. 4(4).

3.5. Overall characteristics of magnetic properties

The obtained basic magnetic properties of pilot samples from each site indicate the reliability of NRM. According to the results of AF demagnetization, stable remanence can be removed from NRM by means of an optimum AF demagnetizing field in the case of all samples. Optimum demagnetizing field intensity is estimated at a peak of 350 Oe and 150 Oe for samples of (14) and elsewhere respectively.

Pilot samples of (3) and (9) show a high value of I_n/I_s , I_s - T curve Type 4 and mainly hematite magnetic minerals. Saturation magnetization (I_s) of hematite at room temperature is 0.37 emu/g, *i.e.* $1/249$, as opposed to that of magnetite. However, the hematite in basaltic samples has a stable, strong NRM. Therefore, the source of the NRM which has a high value of I_n/I_s may be hematite. The existence of hematite in these samples is supported by microscopic observation.

Pilot samples showing Type 2 I_s - T curve of (7), (8) and (11) have an NRM intensity of $1.70 \times 10^{-6} \sim 2.81 \times 10^{-5}$ emu/g. As there is no obvious Curie point above room temperature, these intensities may be weak. As the values of H_c and H_{RC} are $73.5 \sim 129$ Oe and $363 \sim 520$ Oe respectively, the NRM of samples of this type is able to have sufficient stability against AF demagnetization.

The existence of titanomagnetite was observed with a microscope in pilot samples of (6). This is consistent with the results of thermomagnetic analysis. In the case of Type 5, the deduction of the existence of titanomagnetite from the I_s - T curve is not consistent with the results of microscopical observation. This discrepancy may be due to fine titanomagnetite grains having titanomagnetite, whose structure is difficult to identify with a microscope.

In general, pilot samples with ilmenite lamellas in the major titanomagnetite grains, *i.e.* the samples of (2) and the reversed magnetized sample of (14), have high values of H_c and H_{RC} of $128 \sim 205$ Oe and $441 \sim 528$ Oe respectively. Pilot samples with skeletal grains, *i.e.* the samples of (5a), (5b), (10) and (11) also have high values of H_c and H_{RC} , namely $75 \sim 305$ Oe and $152 \sim 510$ Oe respectively.

Usually skeletal grains are observed in rapidly cooled lava in the sea as pillow basalt. As there is no geological evidence of eruption in the sea at the Hut Point

Peninsula, lava with skeletal grains have been formed by rapid cooling by snow or ice.

Since the basic magnetic properties of (5a) and (5b) are very similar and the distance between the two sampling sites is about 200 m in the same volcanic ridge, these lavas may be included in the same lava flow. All pilot samples have a stable component of remanence based on the synthetic basic magnetic properties.

4. Paleomagnetic Discussion

The natural remanent magnetization (NRM) of every sample was measured and it was then demagnetized with optimum AF demagnetization field. As mentioned above, the optimum demagnetizing field intensity was found to be 150 Oe for all samples except those from (14), based on AF demagnetization curves. In the case

Table 3. Paleomagnetic results of Cenozoic McMurdo volcanics.

Sampling site	Demag.	N	R (emu/g)	I	D	K	α_{95}	pLat	pLon
1. Fortress Rocks	0	13	3.44×10^{-3}	-84.2	107.5	40.3	6.6		
	150	13	1.45×10^{-3}	-85.2	118.6	38.8	6.7	-71.4 ^c	139.8 ^c E
2. Observation Hill	0	25	0.97×10^{-4}	84.2	214.1	85.3	3.2		
	150	25	1.00×10^{-3}	85.0	201.0	106.6	2.8	-85.4	116.8 E
3. Crater Hill	0	10	2.62×10^{-3}	-77.8	320.9	145.1	4.0		
	150	10	1.66×10^{-3}	-78.3	322.6	139.2	4.1	-75.2	79.4 W
4. Castle Rock (matrix)	0	3	5.21×10^{-4}	-82.3	6.2	362.1	6.5		
	150	3	3.53×10^{-4}	-80.3	6.8	925	4.1	-83.1	5.1 E
5. Near Scott Hut	0	14	5.93×10^{-3}	-72.8	60.5	31.5	7.2		
	150	14	4.47×10^{-3}	-72.1	58.8	29.8	7.4	-61.7	64.8 E
6. Cape Armitage	0	1	2.30×10^{-3}	77.3	237.4	—	—		
	150	1	1.52×10^{-3}	76.2	239.6	—	—	-67.6	72.3 E
7. Between Cape Armitage and Scott Base	0	6	4.47×10^{-3}	-77.8	303.1	30.6	12.3		
	150	6	3.74×10^{-3}	-78.2	301.0	34.0	11.7	-70.7	103.3 W
8. East side of The Gap	0	7	9.43×10^{-4}	-88.0	298.8	25.1	12.3		
	150	7	2.98×10^{-4}	-88.9	331.7	23.3	12.8	-79.8	172.7 E
9. Half Moon Crater	0	6	3.53×10^{-3}	-59.5	285.2	131.8	5.9		
	150	6	1.97×10^{-3}	-60.8	284.5	130.7	5.9	-43.7	100.0 W
10. Second Crater	0	4	1.91×10^{-3}	-76.8	44.4	228.4	6.1		
	150	4	6.98×10^{-3}	-77.1	44.9	197.7	6.6	-72.0	58.4 E
11. Black Knob	0	6	5.25×10^{-4}	-73.4	290.5	49.6	9.6		
	150	6	1.31×10^{-4}	-73.5	284.1	48.8	9.7	-60.1	110.3 W
12. Cape Royds A	0	28	1.25×10^{-3}	-85.8	225.0	76.9	3.1		
	150	28	0.84×10^{-3}	-85.6	234.4	67.9	3.3	-71.2	171.5 W
13. Cape Royds B	0	48	1.02×10^{-3}	-83.4	84.5	137.7	1.8		
	150	48	0.55×10^{-3}	-82.8	82.8	160.7	1.6	-72.4	112.4 E
14. Taylor Valley	0	41	9.59×10^{-4}	-47.9	163.7	2.0	22.7		
	350	41	8.40×10^{-4}	59.1	158.7	75.8	2.6	-51.5	43.3 W

of samples from (14), a peak of 350 Oe was adopted. Table 3 shows the number of examined specimens (N) collected at the same site, the intensity of NRM (R), the mean inclination (I) and declination (D) of NRM before AF demagnetization (Demag. = 0) and after optimum AF demagnetization, for 14 groups. This table shows the estimate of precision (K), the semiangle of the cone of confidence of 95% probability (α_{95}), the paleolatitude (pLat) and the paleolongitude (pLon) of VGP.

In the case of samples from (5a) and (5b), as mentioned above, both lava flows may be the same as the NRM shows similar magnetic properties and almost the same direction. The sampling site of the lava is called (5) Near Scott Hut in Table 3.

The mean intensity of NRM of these basaltic rocks ranges from 5.21×10^{-4} to 5.93×10^{-3} emu/g for the original NRM and 1.31×10^{-4} emu/g to 4.47×10^{-3} emu/g after AF demagnetization with optimum field. In the case of samples from (7), (8) and (11), individual NRM intensity deviated widely from the mean intensity, *i.e.* from 1.87×10^{-2} to 1.70×10^{-6} emu/g despite of their coming from the same site. The samples from (2) and (6) were magnetized to the reversed polarity. In the case of samples from (14), the main inclination is normal polarity, although it changes to reversed when AF demagnetization is applied. Samples from the other 11 groups are magnetized to normal polarity.

Obtained Quaternary paleomagnetic data collected from the Hut Point Peninsula as summarized in Table 3 will be compared first with the previous data as given in Table 4, where the lava at 250 m north of Scott Base (E) can be considered as practically the same lava as (3), (7) and (8). This paleomagnetic polarity is normal magnetization. The maximum difference in the angle of NRM direction (θ) between (3), (7) and (8) is $\theta = 10.8^\circ$, and the difference in angle of the NRM direction of (E) from that of (3) is $\theta = 13.0^\circ$. Since these deviation angles are of the same order of magnitude as the α_{95} values of the respective rock specimens, it may be concluded that the

Table 4. Previous results of Cenozoic paleomagnetism for Antarctica.

Sampling site	N	$R \times 10^{-3}$ (emu/cc)	I	D	K	α_{95}	pLat	pLon	Refer- ence*
A. North side, Twin Crater	6	6.5	-23	322	870	2.3	-21.4°	53.6° W	1
B. South end, Second Crater	8	4.0	-80	208	537	2.4	-59.3	175.5 W	1
C. South end, Half Moon Crater	1	10.2	-78	61	—	—	-70.7	78.1 E	1
D. Observation Hill, near nuclear power plant	9	2.7	84	319	89	5.5	-67.5	146.1 E	1
E. Flows, 250 m north of Scott Base	9	5.7	-88	196	1836	1.2	-74.0	170.7 E	1
F. Cenozoic volcanics of Cape Hallett (72°S, 171°E)	23		80	208	48	4.2	81	94 E	3
G. Tertiary dykes (Marie Byrd Land)							62	64 E	2
H. Pleistocene volcanics (Marie Byrd Land)							78	128 W	2

* 1: KYLE and TREVES, 1974. 2: SCHARON *et al.*, 1969. 3: TURNBULL, 1959.

mutual agreement of paleomagnetic direction among the four sample groups is reasonably good. The deviation of paleomagnetic direction for the Observation Hill is 9.4° between sample (2) in Table 3 and sample from near the Nuclear Power Plant (D) in Table 4. The main inclination of the samples from the Observation Hill ($I = -84.2$) is almost the same as the mean value of subsurface samples from the Observation Hill Sequence obtained by DVDP 2 (MCMAHON and SPALL, 1974a, b). The deviation value is $\theta = 38.7^\circ$ for (9) and (C) from the Half Moon Crater as compared with Tables 3 and 4. Taking into account the α_{95} values, the two paleomagnetic directions of the Observation Hill are in reasonably good agreement with each other, but the θ value of the Half Moon Crater basalt considerably exceeds their α_{95} values in the two tables. Since sample number $N=1$ for (C) in Table 4, the statistical reliance of the paleomagnetic direction may be considered poor in this case. The lavas from (5a) and (5b), listed together with (5) Near Scott Hut in Table 3, have a similar NRM direction with only 7.3° for the θ value and normal polarity. Their lavas may be considered the same lava group from the viewpoint of field observation, it can be considered the same lava unit. Since the deviation angle (θ) between Fortress Rocks (1) and Cape Royds (13) is 11.3° . As the direction deviation angle is not of the same magnitude as the α_{95} values of the respective sampling sites, individual paleomagnetic directions are statistically significant. Therefore, it is considered that the eruptive sequence of the two lava flows is not exactly the same.

The positions of the VGP of the 14 groups of sites as plotted in Fig. 5 are confined to the polar cap area within 30° colatitude. The previous data on Cenozoic

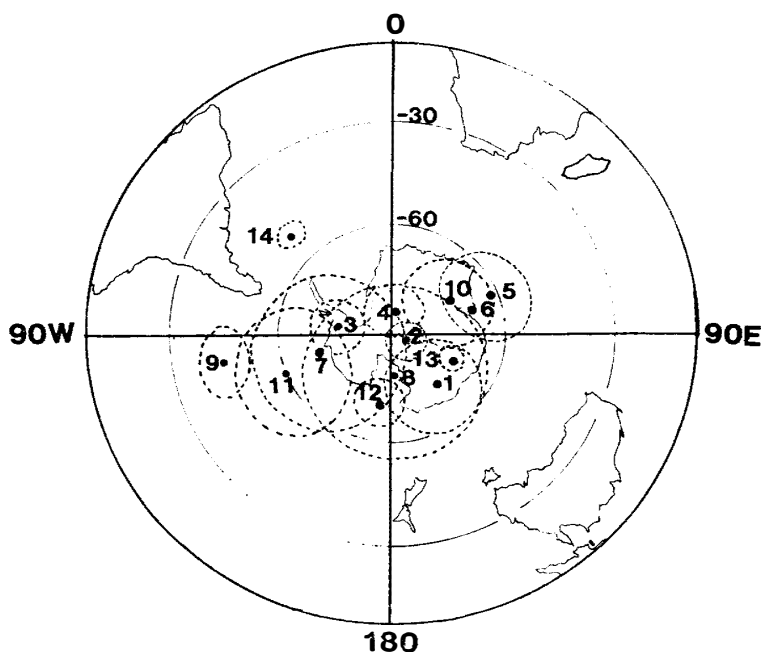


Fig. 5. VGP positions for Hut Point Peninsula from late Pliocene. Equal-area projection. 1. Fortress Rocks. 2. Observation Hill. 3. Crater Hill. 4. Castle Rock. 5. Near Scott Hut. 6. Cape Armitage. 7. Site between Cape Armitage and Scott Base. 8. East side of The Gap. 9. Half Moon Crater. 10. Second Crater. 11. Black Knob. 12. Cape Royds A. 13. Cape Royds B. 14. Taylor Valley.

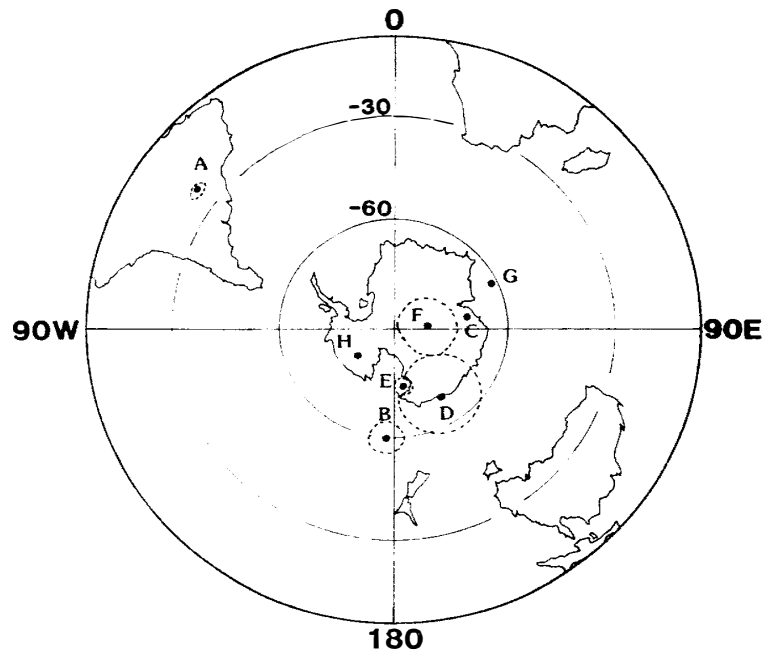


Fig. 6. Previous Cenozoic VGP positions for Antarctica. A~E: VGP from Hut Point Peninsula (KYLE and TREVES, 1974). A; North side, Twin Crater. B; South end, Second Crater. C; South end, Half Moon Crater. D; Observation Hill, near nuclear power plant. E; Flows, 250 m north of Scott Base. F; Cenozoic volcanics of Cape Hallett (TURNBULL, 1959). G and H; Marie Byrd Land (SCHARON *et al.*, 1969). G; Tertiary dykes. H; Pleistocene volcanics.

VGP of Antarctica are plotted in Fig. 6. In Figs. 5 and 6, individual VGP positions are clustered in a wide area in the Southern Hemisphere. In Fig. 6, the latitude of VGP for the samples collected from the north side of the Twin Crater (A) in Table 4 is very low, -21.4° , taking account of α_{95} value compared with other Cenozoic data for Antarctica. From this viewpoint, the NRM direction is anomalous, and probably represents a certain local geomagnetic anomaly.

VGPs from the Plio-Pleistocene to the Quaternary Age in the Northern Hemisphere are clustered quite clearly around the geographic pole rather than the geomagnetic pole, and the mean of the sixty-seven lies at 88.8°N , 131.9°W with α_{95} of 1.9, which is not significantly different from the geographic pole as defined by MCELHINNY (1973). Almost the same results were obtained for Cenozoic volcanics in New Zealand (GRINDLEY *et al.*, 1977) and Reunion Island (CHAMALAUN, 1968) in the Southern Hemisphere. From the viewpoint of sea-floor spread, the Australian continent used to be adjacent to the Australia-Antarctic ridge; during the past 43 m.y. the two continents drifted apart to their present positions (PICHON and HEIRTZLER, 1968). The distance between the Australia-Antarctic ridge and Antarctica is estimated to be about 2000 km. As mentioned above, the oldest samples in this study may be estimated to be 2.9 m.y. old. If the speed of spread of the Antarctic plate is assumed to be 5 cm/year, the normal speed of sea-floor spread, Antarctica was almost exactly in the present position 2.9 m.y. ago. Therefore, the Quaternary VGP of Antarctica are clustered into the narrow area around the south geographic pole. The discrepancy

between this estimation and the obtained result may be due to the high latitude location of the sampling sites, which gives the result that VGP displacement angles δ_i , showing the angular distance between VGP and the present geomagnetic field, are systematically greater in the Southern Hemisphere than in the Northern, and in both hemispheres the standard deviation of δ_i averaged over circles of latitude decreases toward the equator (COX and DOELL, 1964). Based on these viewpoints, the distributions of VGP, as shown in Figs. 5 and 6, do not show exactly the mean VGP positions. However, observed Cenozoic VGP of Antarctica may suggest that the drift area of the geomagnetic field by nondipole field is confined to the polar cap area within a radius of about 30° and the center of the cluster is quite close to the geographical pole.

The historical sequence of lava flow ejections in this area and geomagnetic pole movement will be clarified to a certain extent by synthetically referring to the field

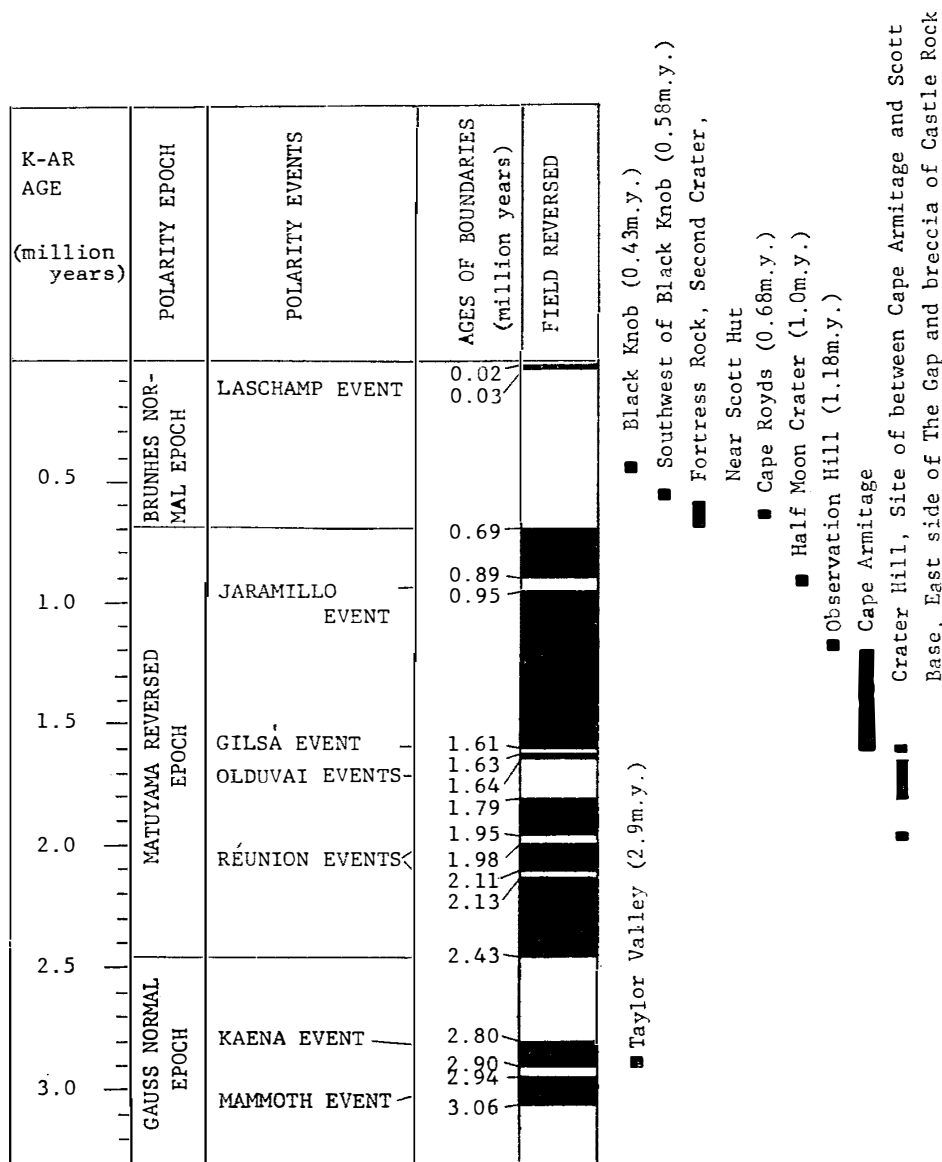


Fig. 7. Eruptive sequence of McMurdo volcanics.

evidence of geological and geochronological data of lava and the present paleomagnetic results. The Black Knob lava, which is 0.43 m.y. in K-Ar age and normal in magnetic polarization, is probably the youngest volcanic rock in the Hut Point Peninsula (WELLMAN, 1964). Lavas from Black Knob, Southwest of Black Knob, Fortress Rock, Scott Hut and Second Crater belong to the Twin Crater Sequence, and all these lavas are normally magnetized. The K-Ar age of the lava from the Southwest of Black Knob has been determined as 0.58 ± 0.06 m.y. (ARMSTRONG, 1978). The lava of Near Scott Hut is under the lava of the Southwest of Black Knob, so that the age of these lavas must be older than 0.58 m.y. The lavas of Fortress Rocks and of Second Crater are older than the Black Knob lavas and are normally magnetized, whence these two lavas are presumed to have flowed out during a period from 0.69 to 0.43 m.y. ago (see Fig. 7). Since the Half Moon Crater lava is 1.0 ± 0.15 m.y. (ARMSTRONG, 1978) in K-Ar age and normally magnetized, it is most likely that the Half Moon Crater volcanic activity took place during the Jaramillo Event, *i.e.*, 0.89 to 0.95 m.y. in age (Cox, 1969), as illustrated in Fig. 7. Both the Observation Hill lava and the Cape Armitage lava gave reverse magnetic polarity. As the K-Ar age of the Observation Hill lava is 1.18 ± 0.03 m.y. (FORBES *et al.*, 1974), its magnetic polarity is in accordance with the world standard paleomagnetic data (Cox, 1969) (Fig. 6). Since the trachyte of the Observation Hill intrudes into Cape Armitage lava at a locality between Observation Hill and the Cape Armitage (KYLE and TREVES, 1974), the Cape Armitage lava should be older than the Observation Hill lava. The Castle Rock palagonitic breccia consists of numerous fragments of large grain size (5 to 20 cm diameter) and the palagonitic matrix; almost tuff including small fragments of basalt less than 5 mm in diameter. The matrix of the Castle Rock breccia is systematically magnetized into the normal direction (Table 3), but the direction of NRM of the large basaltic conglomerates is widely dispersed. The Castle Rock breccia is considered as a subglacial or submarine deposit (KYLE and TREVES, 1974). Then, the most plausible interpretation of the paleomagnetic result of Castle Rock is that this breccia is a product of the deposition of tuff and basaltic materials during a geomagnetic normal polarity epoch 1.1 m.y. ago, resulting thus in an acquisition of DRM or pDRM in the matrix and random orientation of large size conglomerates which were unable to follow the geomagnetic force. It is most likely, from this viewpoint, that the formation of the Castle Rock breccia took place before the Gilsa Event (1.61 to 1.63 m.y. in age) during normal polarity. The Crater Hill lavas are normally magnetized at the top of the Crater Hill and between Cape Armitage and Scott Base. Since these lavas are overlain by the Observation Hill trachyte (KYLE and TREVES, 1974), they must be older than 1.18 m.y. in age. Then, the age of formation of the Crater Hill lavas is presumed to be older than the Gilsa Event for the same reason as applied to the Castle Rock breccia. In general, as the construction of the Hut Point Peninsula seems to be earlier than Pliocene, the lower boundary of the Crater Hill Sequence and the Castle Rock Sequence may be 2 m.y.

Since both kenite lava flows from Cape Royds are magnetized to normal polarity and the estimated age is 0.68 ± 0.14 m.y. (TREVES, 1967). The inferred eruptive sequence is the early Matuyama reversed epoch.

The sampling site of basalt at the Taylor Valley in this study corresponds to the

site for age determination by ARMSTRONG (1978). The obtained ages range from 2.87 ± 0.15 m.y. to 2.93 ± 0.10 m.y. using the K-Ar method. As the NRM direction after AF demagnetization up to 350 Oe shows reversed polarity, the eruptive sequence of basalt from the Taylor Valley can be assigned to the Kaena Event in the Gauss normal epoch as shown in Fig. 7.

5. Concluding Remarks

From the synthetic experimental evidence of basic magnetic properties, it is deduced that all samples from the Hut Point Peninsula, the Cape Royds and the Taylor Valley have a stable component of natural remanent magnetization. The results of paleomagnetic studies of 13 basaltic lavas and one pyroclastic breccia in the McMurdo volcanics since the late Pliocene period are summarized in the VGP distribution chart in Fig. 6 and in the geologic history diagram with a geomagnetic polarity scale in Fig. 7. The ellipse confidence for VGP in Fig. 6 suggests that the positions of VGP are confined to the polar cap area within 46° colatitude, and those of 12 groups (excluding the basaltic samples from the Half Moon Crater and the Taylor Valley) are distributed within a polar cap area of 30° in colatitude. The center of distribution of VGP is in almost the same position on the geographical south pole. It seems, therefore, that Antarctica existed in almost exactly the same position as the present at least by the late Pliocene time. The reason for this distribution of VGP is not continental drift, but is due to the nondipole geomagnetic field. An overall summary of paleomagnetic, geological and geochronological data gives the following time sequence of geologic history in the Hut Point Peninsula, Cape Royds and Taylor Valley, from the latest to the earliest; Twin Crater and Cape Royds (Brunhes Epoch), Half Moon Crater (Jaramillo Event), Observation Hill and Cape Armitage (Matuyama Epoch), Crater Hill and Castle Rock (Olduvai or Réunion Events) and Taylor Valley (Kaena Event).

References

- AKIMOTO, S., KATSURA, T. and YOSHIDA, M. (1957): Magnetic properties of $TiFe_2O_4$ - Fe_3O_4 system and their change with oxidation. *J. Geomagn. Geoelectr.*, **9**, 165-178.
- ANGINO, E. E., TURNER, M. D. and ZELLER, E. J. (1962): Reconnaissance geology of lower Taylor Valley, Victoria Land, Antarctica. *Geol. Soc. Am. Bull.*, **5**, 1553-1562.
- ARMSTRONG, R. L. (1978): K-Ar dating: Late Cenozoic McMurdo volcanic group and dry valley glacial history, Victoria Land, Antarctica. *N. Z. J. Geol. Geophys.*, **21**(6), 685-698.
- CHAMALAUN, F. H. (1968): Paleomagnetism of Reunion Island and its bearing on secular variation. *J. Geophys. Res.*, **73**, 4647-4659.
- COLE, J. W., KYLE, P. R. and NEALL, V. E. (1971): Contributions to Quaternary geology of Cape Crozier, White Island and Hut Point Peninsula, McMurdo Sound region, Antarctica. *N. Z. J. Geol. Geophys.*, **14**(3), 528-546.
- COX, A. V. (1966): Paleomagnetic research on volcanic rocks of McMurdo Sound. *Antarct. J. U. S.*, **1**(4), 136.
- COX, A. (1969): Geomagnetic reversals. *Science*, **163**, 237-245.
- COX, A. and DOELL, R. R. (1964): Long period variations of the geomagnetic field. *Bull. Seismol. Soc. Am.*, **54**(6), Part 8, 2243-2270.
- FORBES, R. B., TUNER, D. L. and CARDEN, J. R. (1974): Age of trachyte from Ross Island, Antarctica. *Geology*, **2**, 297-298.

- FUNAKI, M. (1979): Paleomagnetism of Hut Point Peninsula volcanic Sequence. Mem. Natl Inst. Polar Res., Spec. Issue, **14**, 186–193.
- GRINDLEY, G. W., ADAMS, C. J. D., LUMB, J. T. and WATTERS, W. A. (1977): Paleomagnetism, K-Ar dating and tectonic interpretation of Upper Cretaceous and Cenozoic volcanic rocks of the Chatham Islands, New Zealand. N. Z. J. Geol. Geophys., **20**(20), 425–467.
- HARRINGTON, H. J. (1958): Nomenclature of rock units in Ross Sea region of Antarctica. Nature, **182**, 290.
- KYLE, P. R. and TREVES, S. B. (1973): Review of the geology of Hut Point Peninsula, Ross Island, Antarctica. DVDP Bull., **2**, 1–10.
- KYLE, P. R. and TREVES, S. B. (1974): Geology of Hut Point Peninsula, Ross Island. Antarct. J. U. S., **9**(5), 232–234.
- LARSON, E. E., OZIMA, M., OZIMA, M., NAGATA, T. and STRANGWAY, D. W. (1969): Stability of remanent magnetization of igneous rocks. Geophys. J., **17**, 263.
- MCELHINNY, M. W. (1973): Paleomagnetism and Plate Tectonics. Cambridge, Cambridge University Press, 186.
- MCMAHON, B. and SPALL, H. (1974a): Results of paleomagnetic investigation of selected cores recovered by Dry Valley Drilling Project. DVDP Bull., **4**, 37–38.
- MCMAHON, B. E. and SPALL, H. (1974b): Paleomagnetic data from unit 13, DVDP hole 2. Ross Island. Antarct. J. U. S., **9**(5), 229–232.
- NAGATA, T., FISHER, R. M. and SCHWERER, F. C. (1972): Lunar rock magnetism. Moon, **4**, 169–186.
- PICHON, L. X. and HEIRTZLER, J. R. (1968): Magnetic anomalies in the Indian Ocean and sea-floor spreading. J. Geophys. Res., **73**, 2101–2117.
- SCHARON, L., SHIMOYAMA, A. and SCHARNBERGER, C. (1969): Paleomagnetic investigations in the Ellsworth Land area, Antarctica. Antarct. J. U. S., **4**(4), 94–95.
- TREVES, S. B. (1962): The geology of Cape Evans and Cape Royds, Ross Island, Antarctica. Antarct. Res. Geophys. Monogr., **7**, 40–46.
- TREVES, S. B. (1967): Volcanic rocks from the Ross Island, Marguerite Bay and Mt. Wedver areas, Antarctica. JARE Sci. Rep., Spec. Issue, **1**, 136–149.
- TREVES, S. B. and KYLE, P. R. (1973): Geology of DVDP 1 and 2, Hut Point Peninsula, Ross Island, Antarctica. DVDP Bull., **2**, 11–82.
- TURNBULL, G. (1959): Some palaeomagnetic measurements in Antarctica. Arctic, **12**, 151–157.
- WELLMAN, H. W. (1964): Later geological history of Hut Point Peninsula, Antarctica. Trans. R. Soc. N. Z. Geol., **2**(10), 147–154.

(Received June 23, 1982; Revised manuscript received August 25, 1982)